J Therm Anal Calorim (2012) 107:927–933
DOI 10.1007/s10973-011-1755-7

Prediction of incompatible reaction of dibenzoyl peroxide by isothermal calorimetry analysis and green thermal analysis technology

Jo-Ming Tseng · Chun-Ping Lin

Received: 27 February 2011 / Accepted: 16 June 2011 / Published online: 7 July 2011

Abstract Dibenzoyl peroxide (BPO) has been widely employed in the petrifaction industry. This study determined the unsafe characteristics of organic peroxide mixed with incompatible materials so as to help prevent runaway reactions, fires or explosions in the process environment. Thermal activity monitor III (TAM III) was applied to assess the kinetic parameters, such as kinetic model, reaction order, heat of reaction (ΔH_d), activation energy (E_a), and pre-exponential factor (k_0), etc. Meanwhile, TAM III was used to analyze the thermokinetic parameters and safety indices of BPO and contaminated with sulfuric acid (H_2SO_4) and sodium hydroxide (NaOH). Simulations of a 0.5 L Dewar vessel and 25 kg commercial package in green thermal analysis technology were performed and compared to the thermal stability. From these, the optimal conditions were determined to avoid violent reactions in incompatible materials that cause runaway reactions in storage, transportation, and manufacturing.

Keywords Dibenzoyl peroxide · Incompatible material · Thermal activity monitor III (TAM III) · Thermal hazard · Thermokinetic parameters

J.-M. Tseng
Institute of Safety and Disaster Prevention Technology, Central Taiwan University of Science and Technology, 666, Buzih Rd, Taichung 40601, Taiwan, ROC

C.-P. Lin (✉)
Department of Health and Nutrition Biotechnology, College of Health Science, Asia University, 500, Lioufeng Rd. Wufeng, Taichung 41354, Taiwan, ROC
e-mail: chunping927@gmail.com

List of symbols

C_p	Specific heat capacity (J g^{-1} K^{-1})
CT	Control temperature (°C)
E_a	Activation energy (kJ mol^{-1})
E_1	Activation energy of the 1st stage (kJ mol^{-1})
E_2	Activation energy of the 2nd stage (kJ mol^{-1})
ET	Emergency temperature (°C)
f_i	Kinetic functions of the ith stage; $i = 1, 2, 3$
$f(\alpha)$	Kinetic functions
k_0	Pre-exponential factor (m^3 mol^{-1} s^{-1})
k_i	Reaction rate constant (mol L^{-1} s^{-1}); $i = 1, 2$
n	Reaction order or unit outer normal on the boundary, dimensionless
NC	Number of components, dimensionless
n_i	Reaction order of the ith stage, dimensionless; $i = 1, 2, 3$
Q_i^{∞}	Specific heat effect of a reaction (J kg^{-1})
Q	Heat flow (J g^{-1})
R	Gas constant (8.31415 J K^{-1} mol^{-1})
r_i	Reaction rate of the ith stage (g s^{-1}); $i = 1, 2, 3, 4$
S	Heat-exchange surface (m^2)
SADT	Self-accelerating decomposition temperature (°C)
T	Absolute temperature (K)
T_0	Exothermic onset temperature (°C)
TCL	Time to conversion limit (year)
TCR	Critical temperature (°C)
TER	Total energy release (kJ kg^{-1})
T_e	Ambient temperature (°C)
TMR_{iso}	Time to maximum rate under isothermal conditions (day)
T_{wall}	Temperature on the wall (°C)
T	Time (s)
W	Heat power (W g^{-1})
z	Autocatalytic constant, dimensionless
α	Degree of conversion, dimensionless

γ	Degree of conversion, dimensionless
ρ	Density (kg m^{-3})
λ	Heat conductivity (W m^{-1} K^{-1})
χ	Heat transfer coefficient (W m^{-2} K^{-1})
ΔH_d	Heat of decomposition (kJ kg^{-1})

Introduction

Dibenzoyl peroxide (BPO) is a commercial chemical that is to be transported and stored under low temperature [1–6]. Organic peroxides, which have been widely employed in the chemical industry, have been used to manufacture polymer materials [7]. In terms of manufacturing and international management, many serious explosions and fires are caused because of thermal decomposition and mixing of incompatible materials, such as acids, bases, metal powder, etc. [4]. The goals of this study were to obtain reliably accurate thermokinetic parameters that can be applied to industrial manufacturing processes and incompatible reactions to avoid a reaction disaster.

The thermal activity monitor III (TAM III) [8, 9], a microcalorimeter, was used to detect and record the exothermic activity of BPO under isothermal condition. The aim of this research was to verify the thermokinetics and to establish a simplified model to illustrate the exothermic decomposition of BPO by using an isothermal microcalorimeter to obtain the required data [8, 9].

The chosen approach was to establish a simple, green thermal technology for thermal decomposition that included the thermal hazard and the incompatible reaction properties [7, 10, 11], such as the heat of decomposition (ΔH_d), reaction order (n), activation energy (E_a), isothermal time to maximum rate (TMR_{iso}), time to conversion limit (TCL), self-accelerating decomposition temperature (SADT), control temperature (CT), emergency temperature (ET), the critical temperature (TCR), and total energy release (TER) for a container containing BPO and mixed in incompatible materials.

The SADT is an important parameter for the safe management of reactive substances during storage and transportation [1, 2, 5, 6]. The SADT is generally determined by one of four testing methods recommended in the UN orange book [1, 2, 12–14]: the United States (US) SADT test, the adiabatic storage test, the isothermal storage test, and the heat accumulation storage test [2, 12–22]. The most commonly used tests for organic peroxides are the UN and US SADT tests. The tests were applied to 0.5 L and 25 kg containers. We simulated these methods for thermal hazard evaluation and developed a swift and simple procedure to determine the thermokinetic parameters and the thermal hazard and the incompatible reaction of BPO. The model may be applied to evaluate the incompatible reaction of organic peroxides.

Experimental and methods

Samples

BPO of 75 mass%, a white granule, was purchased from Yuh Tzong Enterprise Ltd., and was stored at normal atmospheric temperature. The original BPO, the BPO mixed in 10 mass% 6 N H_2SO_4 and the BPO mixed in 10 mass% 6 N NaOH were analyzed, respectively, by TAM III tests [8, 9].

TAM III

TAM III was used to investigate a runaway reaction at 80 °C [8, 9]. Approximately 110 mg of the sample was poured into a glass shell (4 mL), and was used for acquiring the experimental data. The absolute temperature could be adjusted to within 0.02 K. While operating in the isothermal mode, the mean bath temperature fluctuations were within 10^{-5} K. The maximum scanning rate was ± 2 K h^{-1} for measuring the chemical and physical equilibrium. The baseline was held at ~ 2 mW. We used the TAM III software to control the thermostat [8, 9]. The thermostat solid is mineral oil with a total volume of 22 L, and the temperature range of the thermostat was 15–150 °C when mineral oil was used [8, 9]. The drift over 24 h was within ± 100 μK. Measurements were conducted isothermally at 80 °C.

Solid thermal explosion simulation

The solid thermal explosion model and the algorithms that were used have been previously described [7, 11]. We used a 0.5 L Dewar vessel and a 25 kg commercial package as the reactor sizes to simulate the solid thermal hazard and incompatible reaction. The radius, width, height, and shell thickness and the reactors were assigned properties as listed in Table 1.

Results and discussion

Determination of thermokinetic parameters by TAM III

Simulations of kinetic models can be complex multi-stage reactions that may consist of several independent, parallel, and consecutive stages [7, 10, 11]:

Table 1 Boundary conditions for 0.5 L Dewar vessel and 25 kg commercial cubic packages

Package shape	Size			Boundary conditions	χ/W m^{-2} K^{-1}	Initial temperature/°C
	Radius/m, width/m	Height/m	Shell thickness/m			
0.5 L vessel	0.0286	0.18	0.00286	Top/3rd kind	1.4567 [21]	20
				Side/3rd kind	1.4567 [21]	
				Bottom/1st kind	–	
25 kg package	0.3	0.3	0.015	Top/3rd kind	2.8386 [21]	20
				Sides/3rd kind	2.8386 [21]	
				Bottom/1st kind	–	

Simple single-stage reaction:

$$\frac{d\alpha}{dt} = k_0 e^{\frac{-E_a}{RT}} f(\alpha) \quad (1)$$

Single-stage for nth-order reaction:

$$\frac{d\alpha}{dt} = k_0 e^{\frac{-E_a}{RT}} (1-\alpha)^n \quad (2)$$

Multi-stage for autocatalytic reaction:

$$f(\alpha) = (1-\alpha)^{n_1}(\alpha^{n_2} + z), \quad (3)$$

where E_a is the activation energy, k_0 is the pre-exponential factor, z is the autocatalytic constant, and n_1 and n_2 are the reaction orders of a specific stage [7, 10, 11].

Reactions that include two consecutive stages:

$$\frac{d\alpha}{dt} = k_1 e^{\frac{-E_1}{RT}} (1-\alpha)^{n_1}; \quad \frac{d\gamma}{dt} = k_2 e^{\frac{-E_2}{RT}} (\alpha-\gamma)^{n_2}, \quad (4)$$

where α and γ are the conversions of the reactant A and product C, respectively. E_1 and E_2 are the activation energies of the stages.

Two parallel reactions for full autocatalysis:

$$\frac{d\alpha}{dt} = r_1(\alpha) + r_2(\alpha); \quad \begin{matrix} r_1(\alpha) = k_1(T)(1-\alpha)^{n_1} \\ r_2(\alpha) = k_2(T)\alpha^{n_2}(1-\alpha)^{n_3} \end{matrix}, \quad (5)$$

where r_1 and r_2 are the rates of each stage and n_3 is the reaction order of stage three.

The kinetic parameters were determined from the TAM III data by isothermal tests holding temperature at 80 °C as displayed in Fig. 1. We hypothesized that the thermal decomposition of BPO represents an unknown reaction, such as an *n*th-order reaction or autocatalytic reaction. We used the *n*th-order and autocatalytic simulations to calculate the thermokinetic parameters. The simulation results are in Table 2.

From comparisons of BPO's *n*th-order reaction simulation, autocatalytic reaction simulation and the literature data, we obtained better results for the thermal explosion parameters with the autocatalytic reaction. In addition, the results of evaluation thermokinetic parameters by autocatalytic kinetic model simulation can be matched in the literature.

Comparisons of the experimental data and the data derived from simulated *n*th-order reaction and autocatalytic

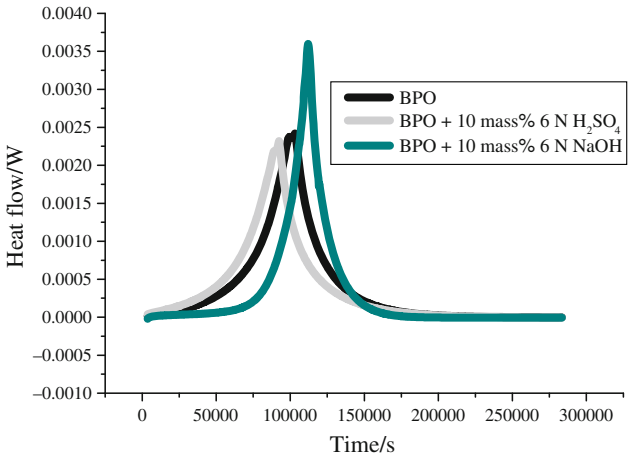

Fig. 1 TAM III thermal curves for original BPO, mixed in H_2SO_4, and mixed in NaOH decomposition with isothermal temperature at 80 °C

reaction for heat production and heat production rate versus time are shown in Figs. 2, 3, 4, 5, 6, and 7. In addition, from comparisons of the autocatalytic thermokinetic parameters of original BPO, mixed in H_2SO_4 and NaOH, the stability of that mixed with NaOH is greater than the original BPO and the mixed with H_2SO_4. Especially, when added in H_2SO_4, the E_a value of thermal decomposition is low and the $\ln k_0$ value of thermal decomposition is high, respectively.

The results showed the BPO added in H_2SO_4 will be dangerous under storage and transportation. This data set was excluded from further analysis. While analyzing the thermokinetic parameters, we acquired three numbers for the autocatalytic thermokinetic parameters for original BPO, mixed in NaOH, and mixed in H_2SO_4, respectively, in the thermal hazard simulation. In addition, we also added literature data to simulate the thermal hazard in this study.

Thermal hazard simulation

To simulate thermal explosions in a solid, the critical parameters for the thermal explosion were determined

Table 2 Comparisons of the thermokinetic parameters for the evaluation of *n*th order and autocatalytic models with literature data

Sample	BPO		BPO + 6 N H_2SO_4		BPO + 6 N NaOH		Literature data
Kinetic model	*n*th order	Autocatalytic	*n*th order	Autocatalytic	*n*th order	Autocatalytic	
$\ln(k_0)/\ln/s^{-1}$	44.45	24.62	21.11	19.97	29.88	28.78	26.84 [22]
E_a/kJ mol^{-1}	165.74	100.16	97.00	84.27	123.38	110.84	103.84 [22]
Reaction order (n)/*n*th	1.036E−08	0.95	0.03	1.51	1.000E−08	1.01	1 [22]
Reaction order (n_1)/auto							
Reaction order (n_2)	N/A	0.98	N/A	1.52	N/A	1.08	N/A
Autocatalytic constant (z)	N/A	2.316E−04	N/A	4.417E−03	N/A	3.137E−05	N/A
ΔH_d/kJ kg^{-1}	987.09	996.56	836.07	854.17	785.71	792.42	1010 [21]

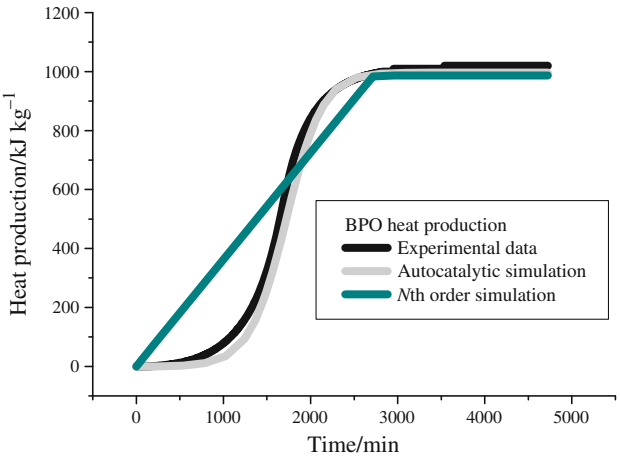

Fig. 2 Original BPO heat production versus time curves of the experimental data, *n*th-order reaction simulation, and autocatalytic simulation

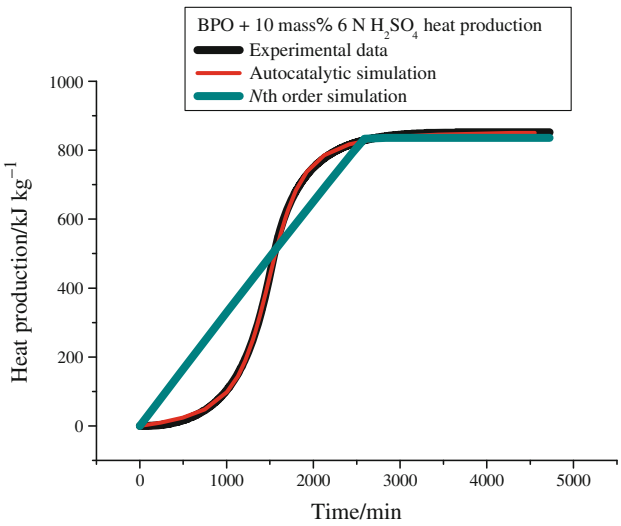

Fig. 4 BPO mixed in H_2SO_4 heat production versus time curves of the experimental data, *n*th-order reaction simulation, and autocatalytic simulation

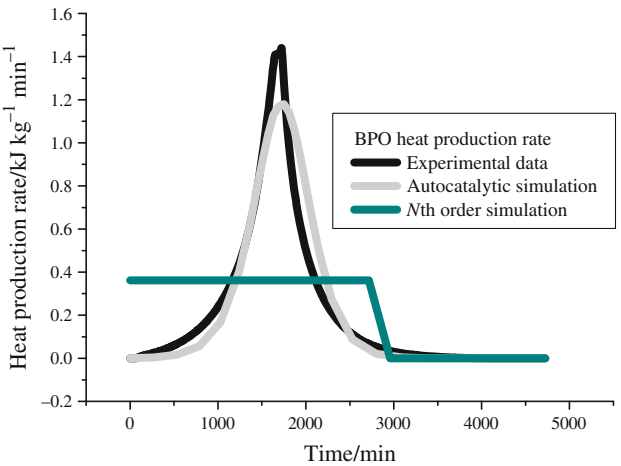

Fig. 3 Original BPO heat production rate versus time curves of the experimental data, *n*th-order reaction simulation, and autocatalytic simulation

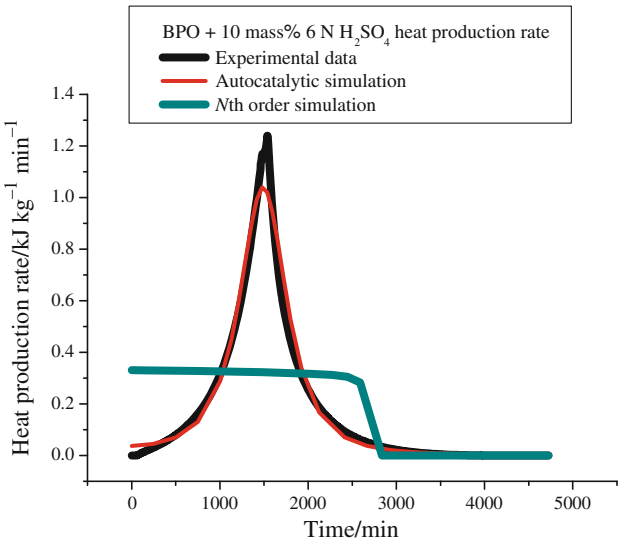

Fig. 5 BPO mixed in H_2SO_4 heat production rate versus time curves of the experimental data, *n*th-order reaction simulation, and autocatalytic simulation

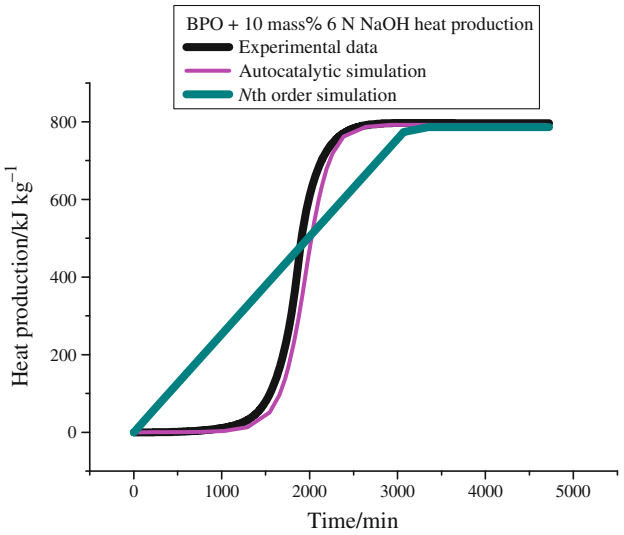

Fig. 6 BPO mixed in NaOH heat production versus time curves of the experimental data, *n*th-order reaction simulation, and autocatalytic simulation

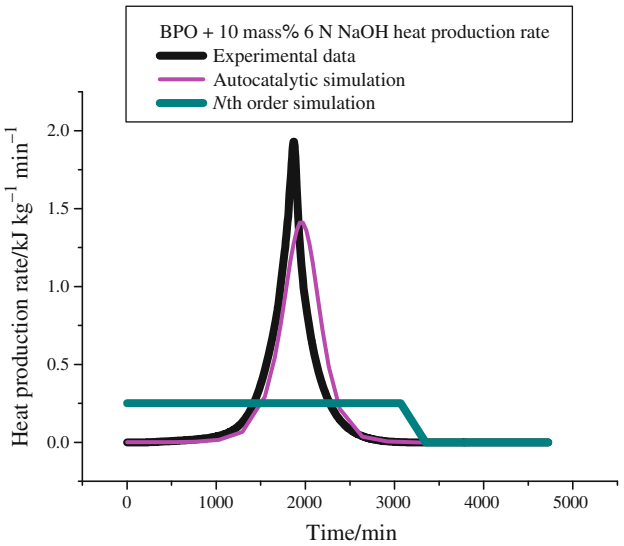

Fig. 7 BPO mixed in NaOH heat production rate versus time curves of the experimental data, *n*th-order reaction simulation, and autocatalytic simulation

numerically from the chemical kinetics for several types of reactor geometries and various boundary conditions, including the possibility to set boundary shells. For solid thermal explosion simulations, the following statements were used [7, 11]:

$$\rho C_p \frac{\partial T}{\partial t} = \mathrm{div}(\lambda \Delta T) + W \tag{6}$$

Thermal conductivity equation

$$\frac{\partial \alpha_i}{\partial t} = r_i, \quad i=1,\ldots \mathrm{NC} \tag{7}$$

Kinetic equations (formal models)

$$W = \sum_{(i)} Q_i^{\infty} r_i \qquad \text{Heat power equation,} \tag{8}$$

where T is the temperature, t is the time, ρ is the density, C_p is the specific heat, λ is the heat conductivity, Q_i^{∞} is the reaction calorific effect, W is the heat power, r is the reaction rate constant, α is the degree of conversion for a component, NC is the number of components, and i is the component number [7, 11].

The initial fields for the temperature and the conversions were constant throughout the reactor volume:

$$\begin{aligned} T|_{t=0} &= T_0 \\ \alpha_i|_{t=0} &= \alpha_{i0} \end{aligned} \tag{9}$$

Here, the index 0 indicates the initial values of the temperature and conversion [7, 11].

The boundary conditions of the first, second, and third kind were specified as:

$$1\text{st kind: } T|_{\mathrm{wall}} = T_{\mathrm{e}}(t) \qquad \text{Temperature} \tag{10}$$

$$2\text{nd kind: } q|_{\mathrm{wall}} = q(t) \qquad \text{Heat flow} \tag{11}$$

$$3\text{rd kind: } -\lambda \left.\frac{\partial T}{\partial n}\right|_S = \chi(T_{\mathrm{wall}} - T_{\mathrm{e}}) \tag{12}$$

Newton′s Colling law.

The indices "wall" and "e" relate to the parameters on the boundary and the environment, respectively. q is the heat flow, and n is the unit outer normal on the boundary [7, 11].

The results of the thermal explosion simulation for the SADT, CT, ET, and TCR are presented in Table 3. The thermal decomposition stability of mixed in 10 mass% NaOH was greater than original BPO, mixed in 10 mass% H_2SO_4 and literature data under lower ambient temperatures. The stability and applicability worsened as the reactor size increased. Here, the TMR_{iso}, TER, and TCL of original BPO, mixed in H_2SO_4 and mixed in NaOH were acquired by simulated autocatalytic kinetic models, as displayed in Figs. 8, 9, and 10.

In contrast to Figs. 8, 9, and 10, the use of simulated autocatalytic kinetic models was proven to give superior results. The TMR_{iso} of original BPO and mixed in NaOH were obtained, which values were ca. less than 30 °C and exceeded the upper limit of 100 days. The TCL of original BPO and mixed in NaOH are less than 30 °C, which is beyond the upper limit of 1 year, but BPO mixed in H_2SO_4 is very dangerous. Especially, Fig. 10 shows the TER of BPO mixed in H_2SO_4 which immediately reaches the maximum heat production.

Table 3 A comparison of the values from the literature and the thermal hazard simulation for SADT, CT, ET, and TCR in the 0.5 L vessel and 25 kg package

Size	Sample	SADT/°C	CT/°C	ET/°C	TCR/°C	SADT/°C in literature
0.5 L	BPO	58	48	53	44	60 [12], 88 [22]
	BPO + 6 N H_2SO_4	53	43	48	41	N/A
	BPO + 6 N NaOH	64	54	59	59	N/A
	Literature data simulation	27	12	17	27	60 [12], 88 [22]
25 kg	BPO	57	47	52	44	>49 [15, 16, 20], 54 [12]
	BPO + 6 N H_2SO_4	50	40	45	37	N/A
	BPO + 6 N NaOH	62	52	57	49	N/A
	Literature data simulation	20	0	10	21	>49 [15, 16, 20], 54 [12]

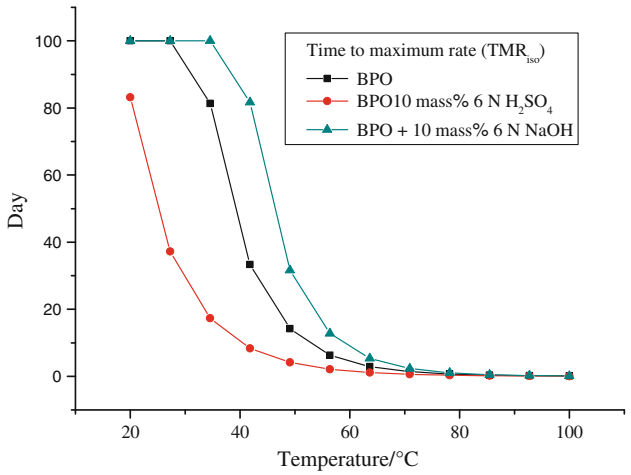

Fig. 8 Simulated time to maximum rate of original BPO, mixed in H_2SO_4, and mixed in NaOH under isothermal conditions

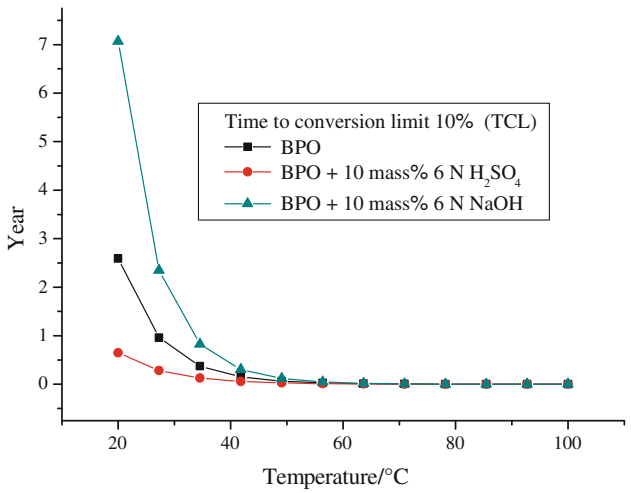

Fig. 9 Simulated time to conversion limit of original BPO, mixed in H_2SO_4, and mixed in NaOH under isothermal conditions

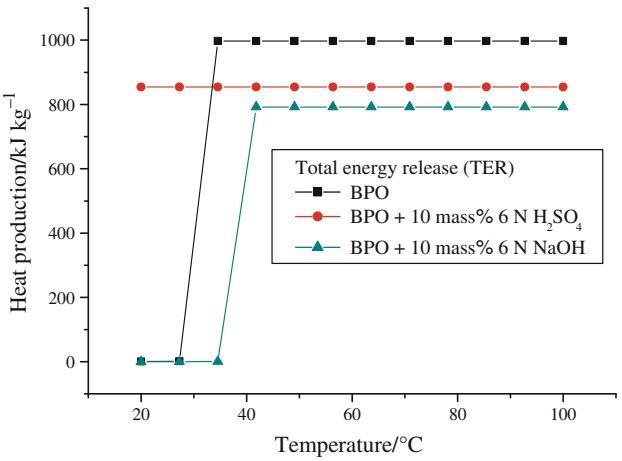

Fig. 10 Simulated total energy release of original BPO, mixed in H_2SO_4, and mixed in NaOH under isothermal conditions

This study developed a swift and simple procedure to determine the thermokinetic parameters and the thermal hazard and the incompatible reaction of BPO. These results could be applied toward energy reduction and safer designs for use and storage. In addition to analyzing the thermal decomposition kinetic parameters through simple isothermal tests and green thermal analysis technology, we found that the results from the green thermal analysis technology presented a reasonable model to calculate the kinetic parameters of thermal decomposition. The validity of the results significantly depends on the reliability of the applied kinetic model, which can be validated by the proper selection of a kinetic model for a reaction and the correctness of the methods used for the kinetics evaluation. The model can be applied to evaluating the incompatible reaction of organic peroxides.

Conclusions

The thermokinetic parameters, from mixing in incompatible materials for the thermal hazard of BPO, were studied

using isothermal calorimetric analysis and green thermal analysis technology. Modeling the thermokinetic and the safety parameters provided precise hazard information concerning the avoidance of thermal accidents during transportation or storage. We developed an effective analysis model for the thermokinetic and thermal hazard parameters of BPO with the simulation method. We also discovered a highly effective and simple way to evaluate the incompatible reaction of BPO.

Acknowledgements The authors are indebted to Prof. Chi-Min Shu and Mr. Shang-Hao Liu for technical suggestions on the experiments and the analysis of the thermal hazardous properties.

References

1. European agreement concerning the international carriage of dangerous goods by road (ADR), United Nations, New York, 2009.
2. Fierz H. Influence of heat transport mechanisms on transport classification by SADT-measurement as measured by the Dewar-method. J Hazard Mater. 2003;96(2–3):121–6.
3. Material Safety Data Sheet, Akzo Polymer Nobel Chemicals, B.V., Stationsplein 77, P.O. Box 247, 3800 AE Amersfoort, The Netherlands, 2010.
4. NFPA 432, Code for the storage of organic peroxide formulations, National Fire Protection Association, Quincy, MA, USA, 2008.
5. Recommendations on the transport of dangerous goods, manual of tests and criteria, 4th rev. ed. United Nations, New York, 2003.
6. Recommendations on the transport of dangerous goods, model regulations, 16th rev. ed. United Nations, New York, 2009.
7. Lin CP, Tseng JM, Chang YM, Liu SH, Shu CM. Modeling liquid thermal explosion reactor containing tert-butyl peroxybenzoate. J Therm Anal Calorim. 2010;102:587–95.
8. The Isothermal Calorimetric Manual for Thermometric AB, 2007, Jarfalla, Sweden.
9. TAM III Thermostat, Product information, 2011, Available at: www.tainstruments.com.
10. Lin CP, Chang YM, Tseng JM, Shu CM. Comparisons of nth order kinetic algorithms and kinetic model simulation on HMX by DSC tests. J Therm Anal Calorim. 2010;100(2):607–14.
11. Lin CP, Chang CP, Chou YC, Chu YC, Shu CM. Modeling solid thermal explosion containment on reactor HNIW and HMX. J Hazard Mater. 2010;176:549–58.
12. Steensma M, Schuurman P, Malow M, Krause U, Wehrstedt KD. Evaluation of validity of the UN SADT H.4 test for solid organic peroxides and self-reactive substances. J Hazard Mater. 2005;A117:89–102.
13. Malow M, Michael-Schulz H, Wehrstedt KD. Evaluative Comparison of Two Methods for SADT Determination (UN H.1 and H.4). J Loss Prev Process Ind. 2010;23:740–4.
14. Malow M, Wehrstedt KD. Prediction of the self-accelerating decomposition temperature (SADT) for solid organic peroxides from differential scanning calorimetry (DSC) measurements. J Hazard Mater. 2005;A120:21–4.
15. Fisher HG, Goetz DD. Determination of self-accelerating decomposition temperatures using the accelerating rate calorimeter. J Loss Prev Process Ind. 1991;4:305–16.
16. Fisher HG, Goetz DD. Determination of self-accelerating decomposition temperatures for self-reactive substances. J Loss Prev Process Ind. 1993;6(3):183–94.
17. Li YF, Hasegawa K. On the thermal decomposition mechanism self-accelerating materials and evaluating method for their SADTs. 9th International Symposium Loss Prevention in the Process Industries, 1998. p. 555–569.
18. Sun JH, Li YF, Hasegawa K. A study of self-accelerating decomposition temperature (SADT) using reaction calorimetry. J Loss Prev Process Ind. 2001;14(5):331–6.
19. Whitmore MW, Wilberforce JK. Use of the accelerating rate calorimeter and the thermal activity monitor to estimate stability temperatures. J Loss Prev Process Ind. 1993;6(2):95–101.
20. Wilberforce JK. The use of the accelerating rate calorimeter to determine the SADT of organic peroxides. Columbia Scientific Corp. Internal report, Texas, 1981.
21. Yang D, Koseki H, Hasegawa K. Predicting the self-accelerating decomposition temperature (SADT) of organic peroxides based on non-isothermal decomposition behavior. J Loss Prev Process Ind. 2003;16(5):411–6.
22. Yu YH, Hasegawa K. Derivation of the self-accelerating decomposition temperature for self-reactive substances using isothermal calorimetry. J Hazard Mater. 1996;45(2–3):193–205.